Catal Lett (2009) 128:235–242
DOI 10.1007/s10562-008-9744-6

Green Conversion of Phenolic Compound to Benzoate Over Polymer-Supported Phase-Transfer Catalysts

Hung-Ming Yang · Chin-Chen Huang

Received: 20 August 2008 / Accepted: 17 October 2008 / Published online: 11 November 2008

Abstract The conversion of sodium phenoxide into benzoates over polymer-supported phase-transfer catalysts with trialkylamines as the functional groups (triphase catalysis) was investigated. The yield of product phenyl benzoate was 100% in 1 h of reaction using a small amount of tributylamine catalyst supported on 1.38% divinylbenzene (DVB) cross-linked copolymer (40–80 mesh) of styrene and chloromethylstyrene. During the reaction, the catalyst stays between the aqueous and organic phases. The overall reaction rate was strongly dependent on the stirring speed and the ionic exchange of Cl^- of the catalyst with PhO^- in the interfacial region. The reaction rate decreased with increasing the mean particle sizes for 1.38% DVB catalyst. The variation of the catalytic intermediate within the catalyst was determined to verify the reaction mechanism. A kinetic model was also proposed to correlate the reaction rate constants. The efficient conversion of phenolic compounds over polymer-supported catalysts shows that triphase catalysis is an efficient green technology in chemical synthesis.

Keywords Esterification · Polymer-supported phase-transfer catalyst · Trialkylamines · Phenyl benzoate · Triphase catalysis

1 Introduction

Phase-transfer catalysis (PTC) is an effective technique in organic synthesis, especially for the reactions of two mutually immiscible reactants. It has been widely applied in synthesizing specialty chemicals, such as pharmaceuticals, perfumes, flavorants, etc. and in environmental control processes for removing harmful pollutants [1, 2]. The reactions conducted by PTC can be divided into several categories including liquid–liquid PTC, solid–liquid PTC, gas–liquid PTC, liquid–liquid–liquid PTC, and solid–liquid–liquid PTC, among which liquid–liquid PTC usually has some problems in the separation of catalyst and products. By using the immobilized phase-transfer catalyst to catalyze the reactions in a liquid–liquid–solid system, those drawbacks can be easily overcome. This type of PTC reactions was also termed as "triphase catalysis" [3, 4]. Although the reactions in triphase catalysis might be limited by the external mass-transfer resistance and/or intraparticle diffusion limitation during the reaction, this type of reactions benefits the subsequent separation of catalyst and cost-saving in process development.

For evaluating the kinetics of reactions by triphase catalysis, Telford et al. [5] suggested an alternating-shell model for the contact of the aqueous and organic phases with the polymer-supported catalyst beads, based on the fact that the apparent catalytic activity varies inversely with the organic volume fraction. Chou and Weng [6] reported the characterization (SEM, EPMA and ESCA) of polymer-supported phase-transfer catalyst, which was prepared by immobilizing tributylamine on chloromethylpolystyrene, and found that the exterior surface of polymer support became wrinkly after immobilization in dry conditions and 46.5% of covalent chloride in chloromethylpolystyrene reacting with tributylamine to form quaternary ammonium chloride. Wang and Yang [7] developed a mathematical model of pseudo-steady-state approach including the considerations of mass transfer of reactants in the bulk phases, the diffusion of reactants

H.-M. Yang (✉) · C.-C. Huang
Department of Chemical Engineering, National Chung Hsing University, 250 Kuo-kuang Road, Taichung 402, Taiwan, ROC
e-mail: hmyang@dragon.nchu.edu.tw

within the catalyst pores, and the intrinsic reactions of the reactants for an etherification conducted in a solid–liquid–liquid system. Desikan and Doraiswamy [8] explored the activity of triphase catalysts for the esterification of benzyl chloride with aqueous sodium acetate, and found that the triphase catalyst has a higher reactivity than its soluble analogs. A kinetic model based on the Langmuir–Hinshelwood and Eley–Rideal types was developed for nucleophilic substitution by considering the reaction rate occurred in the active site of a triphase catalyst to be the rate-limiting step [9]. Wu and Wang [10] investigated the sequential phosphazene reactions by designing two types of continuous flow reactors for conducting the triphase catalysis. Wang et al. [11] conducted the phase-transfer catalyzed etherification of 4,4′-bis(chloromethyl)-1,1′-biphenyl with 1-butanol by polymer-supported catalysis efficiently. Baj et al. [12] investigated the synthesis of dialkyl peroxides in the presence of polymer-supported phase-transfer catalysts with a high yield (60–92%) of the products.

From the past efforts in polymer-supported catalysis, the behavior of the active center within the catalyst was seldom understood. The aim of the present study is to investigate the catalytic activity of polymer-supported phase-transfer catalysts with trialkylamines as the functional groups and the behaviors of catalytic intermediate on esterification of sodium phenoxide into phenyl benzoate in a batch reactor. A kinetic model was proposed to describe the triphase catalysis system.

2 Experimental

2.1 Preparation of Immobilized Phase-transfer Catalysts

Known quantities of gelatin powder, boric acid, calcium carbonate, and NaOH were added into 500 cm^3 of deionized water in a 1,000 cm^3 of four-necked batch reactor. The solution was stirred at 400 rpm, controlled the temperature at the desired values, and sealed by nitrogen. After the reaction temperature reached 90 °C, known quantities of styrene monomer, chloromethylstyrene, divinylbenzene, and 4-methyl-2-pentanol used as the pore template were added into the reactor. The polymerization reaction was then initiated by introducing benzoyl peroxide. After 8 h of reaction, the spherical particles were filtered and washed with 1% NaOH solution six times, and then extracted by acetone in a Soxhlet extractor for 8 h to remove the unreacted components. The porous particles were dried in an oven and used as the catalyst support.

The immobilization of active centers on the polymer support was conducted by reacting trialkylamine with chloromethyl group of the backbone to produce a quaternary ammonium center, denoted as Ⓟ-$CH_3N^+R_3Cl^-$ (Ⓟ-Q^+Cl^-) polymer particles (1.38% DVB, 40–80 mesh, 30.0 g) and trialkylamine (40.0 g) were mixed with 90 cm^3 of dimethylformamide in a 500 cm^3-reactor to react at 65 °C for 3 days. After that, the catalysts were filtered and washed with methanol and acetone in turn for several times, followed by drying under vacuum at 70 °C. The chloride content in the form of Ⓟ-$CH_3N^+R_3Cl^-$ was determined by the Volhard's method. When Cl^- in Ⓟ-$CH_3N^+R_3Cl^-$ was exchanged by PhO^-, the amount of Ⓟ-$CH_3N^+R_3PhO^-$ can be estimated by taking material balance for the active center. The prepared catalysts were then analyzed by BET method and SEM.

2.2 Kinetic Measurements of Triphase Catalysis

Known quantities of benzoyl chloride and diphenylmethane (as the internal standard) were added in a 250 cm^3 of three-necked batch reactor containing organic solvent and kept at the desired temperature. For a batch run, sodium phenoxide in the aqueous phase and the solid catalyst were put into the reactor to start the reaction. The stirring speed was controlled at the desired value. During the reaction, 0.2 cm^3 of organic sample was withdrawn at the chosen time and diluted into 4 cm^3 of acetonitrile. The concentrations of benzoyl chloride and the product phenyl benzoate were analyzed by the internal method using HPLC with a variable-wavelength UV detector at 254 nm, a C-18 (5-μm) column and 1.0 $cm^3\ min^{-1}$ of flow rate of eluent (acetonitrile/water = 70/30 in volume).

3 Kinetic Model

Esterification of sodium phenoxide (PhONa) in the aqueous phase and benzoyl chloride (PhCOCl) in the organic phase was conducted over polymer-supported catalyst. The catalyst would stay in the interfacial region to react with the adsorbed reactants from the aqueous and organic phases. The key catalytic intermediate (Ⓟ-Q^+OPh^-), formed from the ion-exchange reaction of PhONa in the interface and the active sites (Ⓟ-Q^+Cl^-), conducts the intrinsic reaction with the PhCOCl in the interface to produce PhCOOPh. The overall reaction is

$$\mathrm{PhONa_{(aq)}} + \mathrm{PhCOCl_{(org)}} \xrightarrow{PolymerQCl} \mathrm{PhCOOPh_{(org)}} + \mathrm{NaCl_{(aq)}}.$$

The reaction mechanism is shown in the following scheme.

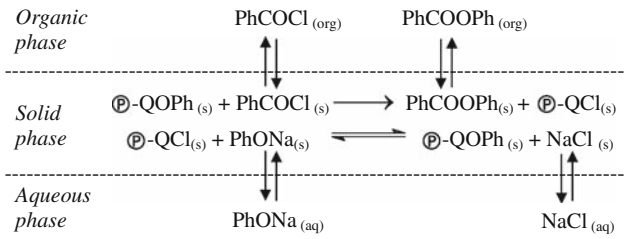

The ionic exchange reaction for forming Ⓟ-QOPh in the solid phase is

$$\text{Ⓟ-QCl}_{(s)} + \text{PhONa}_{(s)} \rightleftharpoons \text{Ⓟ-QOPh}_{(s)} + \text{NaCl}_{(s)}.$$

From experimental results, the amount of Ⓟ-QOPh increased with reaction time, implying that the reverse reaction rate is much slower than that of the forward reaction and can be neglected. With the forward rate constant k_{aq}, the reaction rate of PhONa in the solid phase is

$$-r_{PhONa,s} \cong k_{aq} C_{PhONa,s} \rho_c q_{p-QCl}, \tag{1}$$

where $C_{PhONa,s}$ and q_{p-QCl} represent the concentrations of PhONa in the solid phase and supported Ⓟ-QCl within the catalyst (mmol/g), respectively. The bulk density of catalyst in the reactor is denoted as ρ_c (g/cm^3), and the term $\rho_c q_{p-QCl}$ (mmol/cm^3) represents the local concentration of Ⓟ-QCl available for ionic exchange reaction. The intrinsic reaction of PhCOCl and Ⓟ-QOPh in the solid phase is

$$\text{Ⓟ-QOPh}_{(s)} + \text{PhCOCl}_{(s)} \longrightarrow \text{PhCOOPh}_{(s)} + \text{Ⓟ-QCl}_{(s)},$$

and the rate equation with the rate constant k_{org} is

$$-r_{PhCOCl} = k_{org} C_{PhCOCl,s} \rho_c q_{p-QOPh}, \tag{2}$$

where $C_{PhCOCl,s}$ and q_{p-QOPh} represent the concentrations of PhCOCl in the solid phase and supported Ⓟ-QOPh within the catalyst (mmol/g), respectively. The rate of change of Ⓟ-QOPh at any point of the solid phase is

$$\frac{\partial q_{p-QOPh}}{\partial t} = k_{aq} C_{PhONa,s} q_{p-QCl} - k_{org} C_{PhCOCl,s} q_{p-QOPh}. \tag{3}$$

From the experimental results with excess PhONa, the amount of Ⓟ-QOPh in the solid phase is greatly increased with reaction time, concluding that the production rate of Ⓟ-QOPh is much faster than its consumption rate in Eq. 3; hence, Eq. 3 can be further simplified as

$$\frac{\partial q_{p-QOPh}}{\partial t} \approx k_{aq} C_{PhONa,s} q_{p-QCl} = k_1 q_{p-QCl}, \tag{4}$$

with $k_1 = k_{aq} C_{PhONa,s}$.

The average amount of supported Ⓟ-QOPh or Ⓟ-QCl in the catalyst Q_i is deduced as

$$Q_i = \frac{3}{R^3} \int_0^R r^2 q_i \, dr, \tag{5}$$

where r is the radial position of a spherical particle and R is the particle radius. Thus the rate of change of the average Ⓟ-QOPh in the catalyst is

$$\frac{dQ_{p-QOPh}}{dt} = k_1 Q_{p-QCl}. \tag{6}$$

Taking mass balance for the active sites in the solid phase gives

$$Q_{p-QCl} = Q_{p-QCl,0} - Q_{P-QOPh}, \tag{7}$$

where $Q_{p-QCl,0}$ represents the initial concentration of active sites in mmol/g. Substituting Eq. 7 into Eq. 6, we have,

$$\frac{dQ_{p-QOPh}}{dt} = k_1 (Q_{p-QCl,0} - Q_{p-QOPh}). \tag{8}$$

Integrating Eq. 8 yields the variation of Ⓟ-QOPh on the reaction time,

$$Q_{p-QOPh} = Q_{p-QCl,0}(1 - e^{-k_1 t}). \tag{9}$$

The effect of diffusion within the solid can be expressed by an effectiveness factor η based on the surface concentration of PhCOCl $C^s_{PhCOCl,s}$, and is defined as

$$\eta = \frac{4\pi R^2 D_{PhCOCl} (\partial C_{PhCOCl,s} / \partial r)\big|_{r=R}}{\frac{4}{3}\pi R^3 k_{org} \rho_c Q_{p-QOPh} C^s_{PhCOCl,s}}, \tag{10}$$

where D_{PhCOCl} and $C^s_{PhCOCl,s}$ represent the diffusion coefficient and surface concentration of PhCOCl in the catalyst particle. The reaction rate of PhCOCl in the bulk organic phase (volume V_{org}) is

$$-V_{org} \frac{dC_{PhCOCl}}{dt} = \frac{4}{3}\pi R^3 \eta k_{org} \rho_c Q_{p-QOPh} C^s_{PhCOCl,s} \tag{11}$$

With the mass-transfer coefficient of PhCOCl from the organic phase to the catalyst surface k_m (min^{-1}), the rate of change of PhCOCl in the organic phase is derived as

$$-V_{org} \frac{dC_{PhCOCl}}{dt} = 4\pi R^2 k_m (C_{PhCOCl} - C^s_{PhCOCl,s}) \tag{12}$$

Substituting Eq. 9 into Eq. 11 and combining Eqs. 11 and 12 to solve for $C^s_{PhCOCl,s}$, then the rate of change of PhCOCl in the organic phase can be derived as

$$-\frac{dC_{PhCOCl}}{dt} = k_{app} C_{PhCOCl} (1 - e^{-k_1 t}), \tag{13}$$

where $k_{app} = (\frac{4\pi R^3}{3V_{org}})(\frac{R}{3k_m} + \frac{1}{\eta k_{org} \rho_c Q_{P-QCl,0}})^{-1}$. Inspecting k_{app}, both the mass-transfer factor and intrinsic reaction factor contribute to the apparent reaction rate. Integrating Eq. 13 gives

$$-\ell n\frac{C_{PhCOCl}}{C_{PhCOCl,0}} = k_{app}(t - \frac{1}{k_1}(1 - e^{-k_1 t})). \quad (14)$$

Substituting the product yield $Y = C_{PhCOCl}/C_{PhCOCl,0}$ into Eq. 14, we obtain

$$-\ell n(1 - Y) = k_{app}t - \frac{k_{app}}{k_1}(1 - e^{-k_1 t}). \quad (15)$$

The apparent rate constants k_{app} and k_1 are correlated from the plot of $-\ell n(1-Y)$ versus t by nonlinear regression using least-square method to make a best fit of curve with the least error sum of squares (SSE). The apparent activation energy can also be obtained by applying the Arrhenius' equation $k_{app} = A_0 \exp(-E_{app}/RT)$.

4 Results and Discussion

4.1 Physical Properties of Catalysts

The prepared polymer-supported catalysts were characterized by BET and scanning electron microscopy (SEM), as shown in Table 1 and Fig. 1. From Table 1, the effect of adding pore template 4-methyl-2-pentanol (4M2P) on the immobilization of active center within the triphase catalyst was insignificant, and the chloride contents were determined in the range of 0.92–1.03 mmol/g, slightly lower for the addition of 4M2P than without 4M2P. Moreover, the pore size with 4M2P in the catalyst preparation is larger than that without 4M2P, and their values were approximately 1–2 nm. Figure 1a and b are the SEM images of catalysts with 4M2P for 4.4% and 2.75% of DVB in polymer support, and (c) is the image of catalyst without 4M2P for 1.38% of DVB.

Adding 4M2P in preparing the polymer support makes a larger pore-mouth in the outer surface. The size of such pore-mouth for 2.75% DVB catalyst is about 10 μm in diameter and is larger than that for 4.4% of DVB. Without using 4M2P, the outer surface of the polymer support is relatively smooth with much smaller size of pore-mouth. The structure in outer surface would affect the diffusion of reactants into the interior of the catalyst.

4.2 Effect of Stirring Speeds

In the present reaction system, the catalyst was located in the interfacial region, and the reactants PhONa and PhCOCl mainly diffuse from the aqueous/organic interface into it, indicating that the interfacial mass-transfer resistance would affect the overall reaction rate. Figure 2a is the plot of $-\ell n(1-Y)$ versus time for different agitation speeds, showing the product yield increased with the increase of agitation speed at 15 °C using 0.2 mmol of Ⓟ-Q^+Cl^- and solvent dichloromethane. The upward concave curves indicate that a simple pseudo-first-order kinetic equation cannot be used to describe the overall reaction. The reasons can be explained by the variation of the amount of catalytic intermediate Ⓟ-Q^+OPh^- during the reaction. From the plot of $-\ell n(1-Y)$ versus time, the apparent rate constants k_{app} and k_1 were correlated by applying Eq. 15.

Figure 2b shows the dependence of Ⓟ-QOPh on the reaction time for different agitation speeds, indicating that the overall reaction is substantially controlled by the ionic exchange reaction and the increasing amount of Ⓟ-QOPh. For 200 rpm of stirring speed, almost all of the Ⓟ-QCl sites convert into the active form Ⓟ-QOPh at 60 min of reaction time. The dotted lines in Fig. 2b are the estimated results by the correlated k_1 from Fig. 2a and Eq. 10 and fitted the experimental data well. It demonstrates that the proposed kinetic model can successfully describe the present reaction.

The yield of PhCOOPh in 1 h of reaction, the correlated k_{app} and k_1 for different agitation speeds are shown in Table 2. The product yields for 350–700 rpm all reached 100% and no side reactions were observed, demonstrating that the highly active PhCOCl did not conduct the hydrolysis reaction to produce side-products. The increase in rate

Table 1 Physical properties of the tri-butylamine supported catalysts

Catalyst	% DVB	Particle size[a] (mesh)	Surface area[a] (m^2/g)	Pore volume[a] $\times 10^2$ (cm^3/g)	Pore size[a] (Å)	Cl^- (mmol/g)[b]
With 4M2P	1.38	20–40	0.51	0.049	24.1	0.92
	1.38	40–80	0.62	0.068	22.0	0.97
	1.38	80–120	1.01	0.104	20.6	0.99
	1.38	120–200	1.13	0.113	19.1	0.99
	2.75	40–80	0.68	0.101	29.7	0.94
	4.40	40–80	0.36	0.024	13.6	0.96
Without 4M2P	1.38	20–40	0.41	0.039	15.4	1.05
	1.38	40–80	0.61	0.049	15.7	1.03
	1.38	80–120	0.95	0.077	16.2	1.02
	1.38	120–200	1.00	0.296	14.8	1.03

[a] Determined from N_2 adsorption method and calculated from BET equation

[b] Determined by Volhard's method

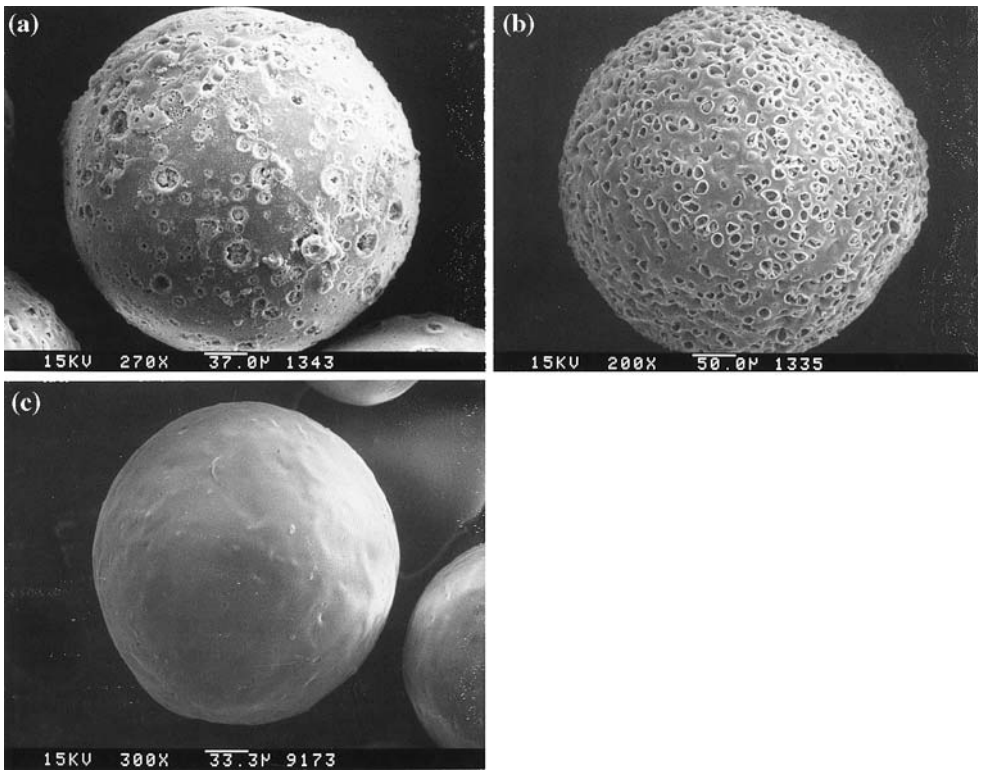

Fig. 1 SEM images of polymer-supported catalyst (40–80 mesh): **a** with 4M2P, 4.4% DVB, **b** with 4M2P, 2.75% DVB, **c** without 4M2P, 1.38% DVB

constants with increasing agitation speed indicates that the external mass-transfer resistance strongly affects this PTC catalyzed esterification. A higher stirring rate would reduce the mass-transfer resistance of the reactants. As noted in Eq. 13, the apparent rate constant k_{app} is affected by mass-transfer coefficient k_m and intrinsic rate constant k_{org}. In this interfacial reaction system, the highly active PhCOCl makes the intrinsic reaction faster and the mass-transfer resistance cannot be neglected at least up to 700 rpm of stirring speed.

4.3 Effect of Functional Groups

The types of functional groups influence the hydrophobic property of the triphase catalyst as well as the intrinsic reactivity and the diffusion rates of reactants. The functional groups employed were triethylamine (TEA), tributylamine (TBA) and trioctylamine (TOA), with decreasing hydrophilicity. Table 3 shows the effect of functional group on the apparent reaction rate constant k_{app}, and k_1.

Using 0.031 mmol of catalyst prepared without 4M2P, the order of activity at 300 rpm was TBA > TOA > TEA; while with 4M2P, the order changes to TOA ≈ TBA > TEA. Without larger open pore-mouth, the more hydrophilic TEA makes the catalyst surface more hydrophilic to retard the organic reactant diffusing into the catalyst. In addition, the less hydrophilic TOA results in a relatively slower rate of ion-exchange reaction to reduce the overall reaction rate. With 4M2P, the larger pores on the outer surface compensate the hydrophobic property of TOA, and thus enhance the diffusion and reaction rate. Apparently, a triphase catalyst with moderate hydrophilic property of functional group and larger pores on the outer surface would have the better catalytic activity. Figure 3a is the plot of $-\ell n(1-Y)$ on the reaction time for TEA, TBA and TOA using 0.2 mmol of Ⓟ-QCl with 4M2P at 15 °C, showing that the order of catalytic activity at 150 rpm was TBA > TOA > TEA. This phenomenon can be explained by the competition of three effects, i.e. hydrophilicity, diffusion rate, and reaction rate. For TOA catalyst with 4M2P at a lower temperature, the effect of less hydrophility of TOA cannot be well compensated by the larger open pores because of the diffusion rate and the ionic reaction rate of PhONa are much lower at a low temperature than that for TBA catalyst. While for TEA catalyst, the higher hydrophilicity makes the diffusion rate and reaction rate of PhCOCl much lower than that of TOA. The interaction of the three effects resulted in the order of reactivity at a low temperature to be TBA > TOA > TEA. The upward concave curves of pseudo-first-order kinetics represent the gradual increase of rate constant on the reaction time. When a larger amount of active center is applied at a lower reaction temperature, the moderate hydrophilic property of TBA favors the interfacial reaction. The observation of nonlinear curves of $-\ell n(1-Y)$ on the

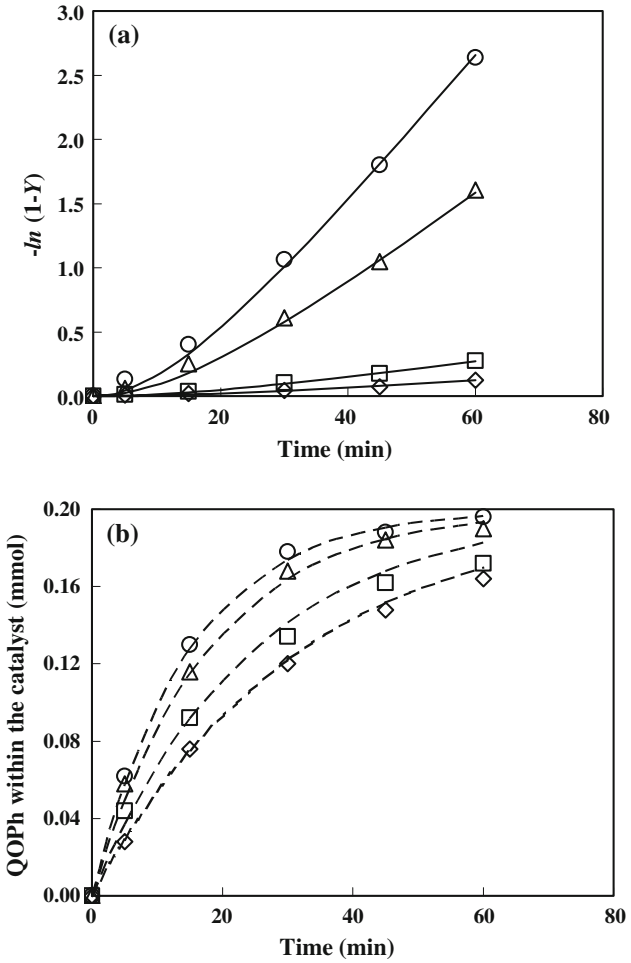

Fig. 2 Effect of agitation speed on (**a**) $-ln(1-Y)$ versus time, (**b**) QOPh within the catalyst versus time, dotted lines: calculation results; sodium phenoxide 6.25 mmol, benzoyl chloride 5 mmol, catalyst (with 4M2P, 40–80 mesh, TBA, 1.38% DVB) 0.2 mmol, water 50 cm^3, dichloromethane 50 cm^3, 15 °C; agitation speed: (◇) 50 rpm, (□) 100 rpm, (△) 150 rpm, (◯) 200 rpm

reaction time can also be described by the variation of Ⓟ-QOPh with time, as shown in Fig. 3b. The amount of Ⓟ-QOPh increased with time in the order of TBA > TOA > TEA, corresponding to the order in the catalytic activity. After 60 min of reaction, above 90% of Ⓟ-QCl was ion-exchanged into Ⓟ-QOPh for TBA.

4.4 Effects of Particle Sizes and Degree of Cross-linking

The particle size of a catalyst and the degree of cross-linking of polymer support affect the external mass-transfer rate, internal diffusion rate and the intrinsic reaction rate of the reactants. Figure 4a shows the dependence of apparent rate constants k_{app} on the reciprocal of mean catalyst size of 20–40, 40–80, 80–120 and 120–200 mesh for different degrees of cross-linking. The apparent reaction rate

Table 2 Effect of agitation speeds on the apparent reaction rate

Stirring speed (rpm)	$k_{app} \times 10^2$ (min^{-1})	k_1(min^{-1})	Yield of PhCOOPh in 1 h of reaction (%)
50[a]	0.179	0.113	17.7
100[a]	0.219	0.121	27.7
150[a]	0.516	0.126	35.2
200[a]	1.23	0.131	69.8
250[a]	1.61	0.145	76.2
300[a]	2.79	0.153	94.7
350[a]	4.15	0.161	100
500[a]	5.86	0.178	100
700[a]	8.06	0.192	100
50[b]	0.373	0.0315	11.8
100[b]	0.678	0.0408	24.1
150[b]	3.69	0.0569	79.9
200[b]	5.81	0.0687	92.8

Conditions: sodium phenoxide 6.25 mmol, benzoyl chloride 5.0 mmol, catalyst (40–80 mesh, tri-butylamine, 1.38% DVB), water 50 cm^3, organic solvent 50 cm^3

[a] Catalyst 0.031 mmol, dichlorobenzene at 25 °C

[b] Catalyst 0.2 mmol, dichloromethane at 15 °C

Table 3 Effect of functional groups on the apparent reaction rate

Types of catalyst	Functional groups	k_{app}(min^{-1})	k_1(min^{-1})
Without 4M2P	TEA[a]	0.0139	0.1026
	TBA[a]	0.0291	0.0659
	TOA[a]	0.0208	0.0625
With 4M2P	TEA[a]	0.0285	0.0625
	TBA[a]	0.0576	0.0929
	TOA[a]	0.0597	0.0711
	TEA[b]	0.0186	0.0315
	TBA[b]	0.0369	0.0569
	TOA[b]	0.0290	0.0461

Conditions: sodium phenoxide 6.25 mmol, benzoyl chloride 5.0 mmol, water 50 cm^3, dichloromethane 50 cm^3; 1.38% DVB and 40–80 mesh catalyst

[a] Catalyst 0.031 mmol, 300 rpm and 25 °C

[b] Catalyst 0.2 mmol, 150 rpm and 15 °C

increased with decreasing particle size significantly for 1.38% of DVB; thus the reaction was strongly controlled by the diffusion owing to the catalyst particles swelled greatly for 1.38% of DVB. As the degrees of cross-linking in catalyst were at 2.75% and 4.4% of DVB (the less swelled particles in organic solvent), the reaction rates were only slightly limited by the particle size. The reactions are conducted near the outer surface of the catalyst under much severe diffusion resistance. Consequently, the reaction rate increased with the decrease of % DVB.

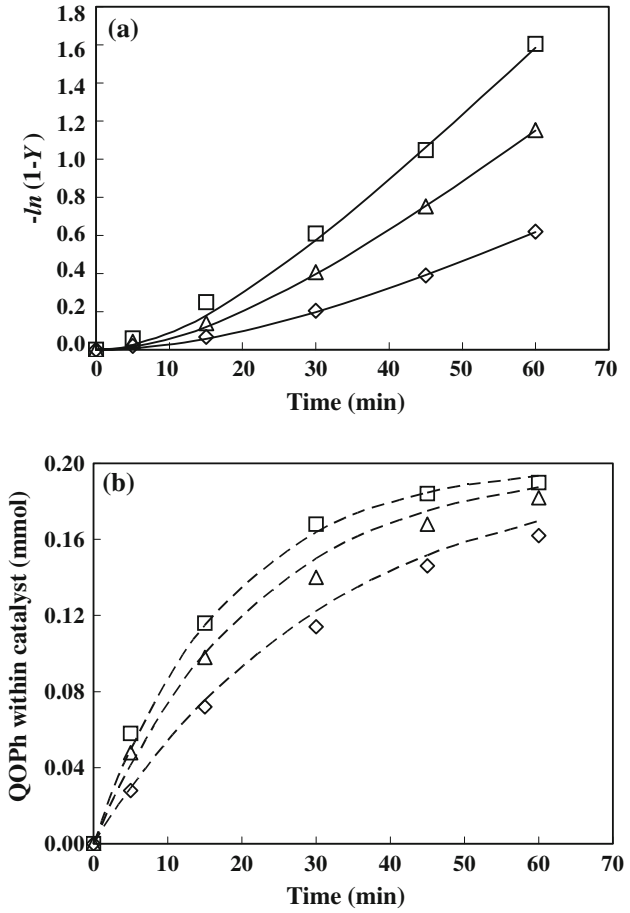

Fig. 3 Effect of functional groups on **a** $-ln(1-Y)$ versus time, **b** QOPh within the catalyst versus time, dotted lines: calculation results; sodium phenoxide 6.25 mmol, benzoyl chloride 5 mmol, catalyst (with 4M2P, 40–80 mesh, TBA, 1.38% DVB) 0.2 mmol, water 50 cm^3, dichloromethane 50 cm^3, 150 rpm, 15°C; (◇) triethylamine, (□) tributylamine, (△) trioctylamine

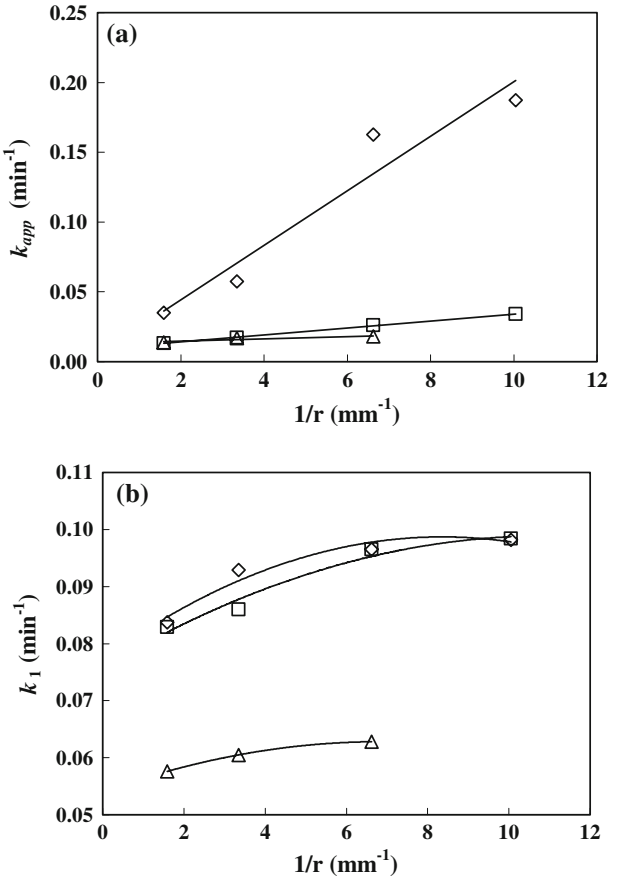

Fig. 4 Effect of catalyst particle size for different degrees of crosslinking, **a** k_{app} versus $1/r$; **b** k_1 versus $1/r$; sodium phenoxide 6.25 mmol, benzoyl chloride 5 mmol, catalyst (with 4M2P, TBA) 0.031 mmol, water 50 cm^3, dichloromethane 50 cm^3, 300 rpm and 25 °C; degree of crosslinking (% DVB): (◇) 1.38, (□) 2.75, (△) 4.4

The similar trends for k_1 were also observed, as shown in Fig. 4b.

4.5 Effects of Amounts of Catalyst and Aqueous Reactant

The amount of active center influences the effective concentration of catalytic intermediate within the catalyst. During the progress of reaction, the catalyst almost stays between the aqueous and organic phases. Using the catalyst of 1.38% DVB (prepared with 4M2P, immobilized with TBA, 40–80 mesh) to conduct the reaction, the dependence of apparent rate constants on the amount of catalyst are shown in Fig. 5. As the amount of Ⓟ-QCl within the catalyst increased from 0.031 to 0.5 mmol, the apparent rate constant k_{app} (min^{-1}) increased from 0.0576 to 0.2584, for which 100% of product yield was obtained in 20 min of reaction. However, the dependence of k_{app} on the amount

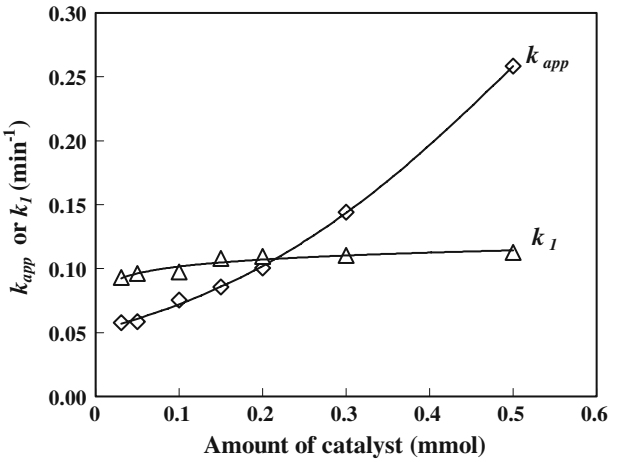

Fig. 5 Effect of the amount of catalyst on k_{app} and k_1; sodium phenoxide 6.25 mmol, benzoyl chloride 5 mmol, catalyst (with 2M4P, 40–80 mesh, TBA, 1.38% DVB), water 50 cm^3, dichloromethane 50 cm^3, 300 rpm and 25 °C

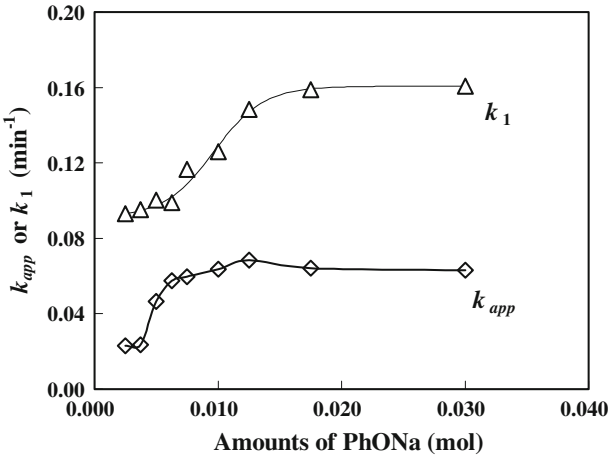

Fig. 6 Effect of the amount of sodium phenoxide on the apparent rate constant; benzoyl chloride 5 mmol, catalyst (with 4M2P, 40–80 mesh, TBA, 1.38% DVB) 0.031 mmol, water 50 cm^3, dichloromethane 50 cm^3, 300 rpm and 25°C

of catalyst is not linear, but with a concave increase. This implies the effective amount of catalytic intermediate Ⓟ-QOPh is greater for a higher initial usage of Ⓟ-QCl. While the rate constants k_1 for different amounts of Ⓟ-QCl within the catalyst vary not much because the adsorbed PhONa in the interface is in its saturation.

Figure 6 shows the plots of k_{app} and k_1 for the effect of PhONa. The reaction rate drastically increased from 3.75 to 12.5 mmol of PhONa because of the rate of ion-exchange reaction increased to produce much more catalytic intermediate, and then kept almost constant when the amount of PhONa was greater than 12.5 mmol due to the saturation of PhONa in the interface.

4.6 Effect of Temperature

Table 4 shows the effect of temperature for different functional groups and preparation method. Using the 1.38% DVB catalyst prepared with 4M2P and TBA, the product yields at 20 and 30 °C were 91.4% and 100% in 1 h. The apparent activation energy was calculated by Arrhenius' plot as 5.13 kcal/mol for 1.38% DVB, which was much lower than that using TEA and TOA. Hence, the mass-transfer-control reaction for using TBA was observed, and the more hydrophilic TEA and more hydrophobic TOA would lead to a reaction-control mechanism. Without adding 4M2P, the apparent activation energy decreased with the increasing hydrophilicity from TOA to TEA, indicating that the increasing importance of mass-transfer effect from TOA to TEA. In addition, the activation energies of 9.93 kcal/mol for 2.75% DVB, and 9.81 kcal/mol for 4.4% DVB show the increasing importance of reaction control.

Table 4 Effect of different of functional groups and % DVB on E_a^a

Types of catalyst	Functional groups	% DVB	E_a (kcal/mol)
With 4M2P	TEA	1.38	13.31
	TBA	1.38	5.13
	TBA	2.75	9.93
	TBA	4.40	9.81
	TOA	1.38	12.76
Without 4M2P	TEA	1.38	7.76
	TBA	1.38	9.68
	TOA	1.38	10.48

[a] Conditions: sodium phenoxide 6.25 mmol, benzoyl chloride 5.0 mmol, catalyst (40–80 mesh) 0.031 mmol, water 50 cm^3, dichloromethane 50 cm^3 and 300 rpm

5 Conclusion

A green synthesis of phenyl benzoate from esterification of benzoyl chloride with sodium phenoxide over polymer-supported phase-transfer catalysts was conducted in a batch reactor. The polymer support was prepared with or without pore template, which influences the catalytic activity. The types of trialkylamine as the functional group of the polymer-supported catalyst show different catalytic activities due to the effect of hydrophilic property. The catalyst was located between the aqueous and organic phases during the reaction, leading to the importance of interfacial ion-exchange reaction and stirring speeds. The variation of catalytic intermediate was determined to verify the reaction controlling regime. A kinetic model for triphase catalysis was successfully applied in the present reaction system.

Acknowledgments The authors acknowledge the financial support of the National Science Council, Taiwan, Republic of China (Grant No. NSC 93-2214-E-005-001). This work is also supported in part by the Ministry of Education, Taiwan, ROC, under the ATU plan.

References

1. Starks CM, Liotta C, Halpern M (1994) Phase transfer catalysis fundamentals application and industrial perspectives. Chapman & Hall, New York
2. Sasson Y, Neumann R (eds) (1994) Handbook of phase transfer catalysis. Chapman & Hall, New York
3. Regen SL (1975) J. Am Chem Soc 97:5956
4. Regen SL, Bolikal D, Barcelon C (1981) J Org Chem 46:2511
5. Telford S, Schlumt P, Chau PC (1986) Macromolecules 19:2435
6. Chou SC, Weng HS (1990) J Appl Polymer Sci 39:1665
7. Wang ML, Yang HM (1991) Ind Eng Chem Res 30:2384
8. Desikan S, Doraiswamy LK (2000) Chem Eng Sci 55:6119
9. Justinus AB, Glatzer HJ, Doraiswamy LK (2000) Chem Eng Sci 55:5013
10. Wu HS, Wang CS (2003) Chem Eng Sci 58:3523
11. Wang ML, Lee ZF, Wang FS (2005) Ind Eng Chem Res 44:5417
12. Baj S, Siewniak A, Socha B (2006) Appl Catal A Gen 309:85